Advances in Aircraft and Spacecraft Science, *Vol. 7, No. 5 (2020) 405–423*
DOI: http://doi.org/10.12989/aas.2020.7.5.405

Aircraft wings dynamics suppression by optimal NESs designed through an Efficient stochastic linearisation approach

Giacomo Navarra*, Francesco Lo Iacono[a], Maria Oliva[b] and Antonio Esposito[c]

Faculty of Engineering and Architecture, Kore University of Enna, Cittadella Universitaria, Enna, Italy

(Received December 31th, 2019, Revised May 16th, 2020, Accepted May 18th, 2020)

Abstract. Non-linear energy sink (NES) is an emerging passive absorber able to mitigate the dynamic response of structures without any external energy supply, resonating with all the modes of the primary structure to control. However, its inherent non-linearities hinder its large-scale use and leads to complicated design procedures. For this purpose, an approximate design approach is herein proposed in a stochastic framework. Since loads are random in nature, the stochastic analysis of non-linear systems may be performed by means of computational intensive techniques such as Monte Carlo simulations (MCS). Alternatively, the Stochastic Linearisation (SL) technique has proven to be an effective tool to investigate the performance of different passive control systems under random loads. Since controlled systems are generally non-classically damped and most of SL algorithms operate recursively, the computational burden required is still large for those problems that make intensive use of SL technique, as optimal design procedures. Herein, a procedure to speed up the Stochastic Linearisation technique is proposed by avoiding or strongly reducing numerical evaluations of response statistics. The ability of the proposed procedure to effectively reduce the computational effort and to reliably design the NES is showed through an application on a well-known case study related to the vibrations mitigation of an aircraft wing.

Keywords: Non-linear Energy Sink; stochastic linearisation; spectral moments

1. Introduction

In the last decades, the constant advances in manufacturing and materials technologies have led to design structures increasingly flexible and lightweight that, however, turn out to be vulnerable to dynamic load and consequently can exhibit excessive vibration responses. In aerospace engineering, the instabilities are often produced by aeroelastic flutters, i.e. self-oscillating phenomena resulting from the interaction between a structure and the surrounding flow, but also by non-linearities in the system leading undesirable limit-cycle oscillations

*Corresponding author, Ph.D., E-mail: giacomo.navarra@unikore.it
[a]Ph.D., E-mail: francesco.loiacono@unikore.it
[b]Ph.D., E-mail: maria.oliva@unikore.it
[c]Ph.D., E-mail: antonio.esposito@unikore.it

http://www.techno-press.org/?journal=aas&subpage=7 ISSN: 2287-528X(Print), 2287-5271(Online)

(LCOs) (Hubbard *et al.* 2010). Since both phenomena in severe cases may lead to failure, great attention has been given to developing strategies able to mitigate or avoid them.

In order to reduce the dynamic response of structural flexible systems subjected to random loads, passive control absorbers are often used. These devices are the most extensively researched and widely used across the world because of their capacity to enhance energy dissipation in the controlled structures without any external supply to trigger the damping process. However, the classical absorbers, such as tuned mass dampers, have a limited control capacity since they are generally tuned to a single structural natural frequency, being effective within a narrow frequency band and very sensitive to the detuning problem. Recently, Non-linear Energy Sinks (NESs) have attracted the attention of researchers because of their capability to passively absorb a significant amount of energy over a wide range of frequencies, thus overcoming the limitations of the classical absorbers (Vakakis *et al.* 2009).

Basically, a NES is prefigured as small mass coupled to the main structure with an essentially non-linear spring, which enables the NES to resonate with any mode of the primary system, and a linear viscous damping element, which dissipates the vibrational energy transferred through resonant modal interactions. An additional feature is its ability to passively and irreversibly absorb from the primary structure a significant amount of energy, that remains confined in the NES and locally dissipated in its damper. This phenomenon is known as passive Targeted Energy Transfer (TET) and it is realised mainly via a p:k resonance capture. The TET has been widely investigated both analytically (Gendelman *et al.* 2001, Vakakis 2001, Gendelman 2001, Kerschen *et al.* 2005, Lee *et al.* 2005, Vakakis *et al.* 2009) and experimentally (Nucera *et al.* 2007, 2008, McFarland *et al.* 2005, Kerschen *et al.* 2007, Gourdon *et al.* 2007, Wang *et al.* 2015a) in different fields of application, such as aerospace, civil and mechanical engineering (Lee *et al.* 2008a).

Application of TET for suppressing LCOs in the van der Pol oscillator is reported in Lee *et al.* (2006), whereas the capacity of single as well as multiple NESs to prevent aeroelastic instabilities occurring in in-flow wings is investigated both theoretically and experimentally in Lee *et al.* (2007a, b, 2008b). It has been demonstrated that a series of transient or sustained resonance captures between the NESs and aeroelastic modes (i.e. pitch and heave modes) suppresses the triggering mechanism that allows LCOs to occur, thus assuring instability-free dynamics.

In (Bergeot *et al.* 2016) the Ground Resonance phenomenon, a dynamic instability involving the coupling of the blades motion in the rotational plane and the helicopter fuselage motion, has been studied and mitigated in a helicopter by using a NES.

In Hubbard *et al.* (2010), the effectiveness of a NES to quickly and efficiently absorb energy from one or more wing modes is investigated. A series of ground-vibration tests have been performed on a system consisting of a uniform-thickness swept wing coupled with a compact NES located at the mid-chord of the wingtip. It has been shown that a NES can be designed to target a specific mode of the wing and to induce strong non-linearity in the specific frequency range of interest.

Due to the non-linear nature of the NES, its design is not an easy task and, consequently, its real scale use is limited. In this paper, an approximate approach to design NESs is proposed in a stochastic framework by using an Efficient Stochastic Linearisation. In the case

of linear systems, the stochastic analysis allows for a straightforward probabilistic characterization of the structural response. Indeed, when referring to non-linear systems, this type of analysis is not directly applicable and is often performed via Monte Carlo simulations, involving a great computational effort. Therefore, taking advantage of the stochastic analysis, it is common to replace the non-linear equations of motion of a controlled system with linear equivalent ones by using well-established procedures as Stochastic Linearisation (SL) techniques (Roberts and Spanos 2003, Atalik and Utku 1976, Elishakoff 2000). However, depending on the parameters of the linear equivalent system implicitly on response statistics, most SL algorithms operate recursively and the computational burden may still large, even if drastically reduced with reference to Monte Carlo simulations. Moreover, calculations are very often carried out only numerically, since analytical closed-form solutions for response statistics are available just for a limited class of problems (Artale *et al.* 2017).

In this work, a procedure to further reduce the computational time of SL techniques is proposed. It can be applied for both classically and not-classically damped systems, and allows for the evaluation of the response spectral moments by avoiding intensive use of numerical calculations. Spectral moments have well-known physical meanings (Vanmarcke 1972, Di Paola and Muscolino 1986): zero-order and second-order spectral moments are the variances of the response and of its time derivatives, respectively; other quantities, namely central frequency and bandwidth parameter, as well as approximate solutions for the first-passage problem can be evaluated in terms of the first spectral moments (Vanmarcke 1975, Der Kiureghian 1980). The proposed procedure essentially consists of following three steps:

1. Evaluation of few first direct spectral moments of modal oscillators. This evaluation may be carried out analytically for certain classes of input Power Spectral Density (PSD) functions (Barone *et al.* 2019);
2. Computation of the cross spectral moments in modal decoupled space (Di Paola and Muscolino 1988);
3. Analytical evaluation of first spectral moments of a set of response quantities of interest, obtained as linear combinations of the selected degrees-of-freedom (Igusa *et al.* 1984).

In the following, the equations of motion and the application of SL technique to the case of Multi-Degree-of-Freedom (MDOF) systems controlled by several NES devices are firstly presented. Then, the Efficient Linearisation Technique is explained in detail. Finally, the last section is devoted to the design of a NES device attached to the tip of an aircraft wing by making use of the proposed method.

2. Mathematical formulation of the NES

2.1 Governing equations

Among the several configurations of NES proposed in literature (Sapsis *et al.* 2012, Gendelman *et al.* 2011, Nucera *et al.* 2007, Gendelman 2008, Gendelman *et al.* 2012, Sigalov *et al.* 2012, Wang *et al.* 2015b), in the following the so-called type-I NES is considered. It consists of a small mass coupled to the main structure through an essentially non-linear

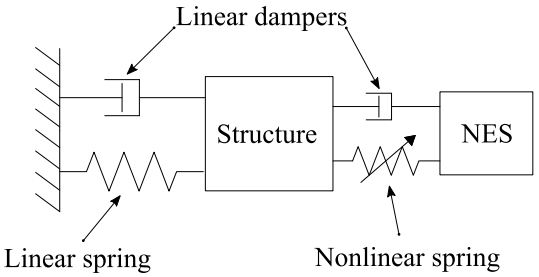

Fig. 1 Schematic representation of a structure controlled by a NES

spring with a cubic stiffness and a linear viscous damping element. The non-linear spring enables the device to resonate with any mode of the primary system, whereas the damping element dissipates the vibrational energy.

Figure 1 shows a schematic representation of the simplest possible case, i.e. a linear SDOF oscillator, representing the structure or its fundamental mode of vibration, coupled to a single type-I NES, whose equations of motion are given as:

$$\begin{cases} m_1\ddot{x}_1(t) + c_1\dot{x}_1(t) + k_1x_1(t) + c_{NES}\left(\dot{x}_1(t) - \dot{x}_{NES}(t)\right) + k_{NES}\left(x_1(t) - x_{NES}(t)\right)^3 = 0 \\ m_{NES}\ddot{x}_{NES}(t) + c_{NES}\left(\dot{x}_{NES}(t) - \dot{x}_1(t)\right) + k_{NES}\left(x_{NES}(t) - x_1(t)\right)^3 = 0 \end{cases} \tag{1}$$

in which m_1, c_1, k_1 are mass, viscous damping and stiffness coefficients of the primary structure and m_{NES}, c_{NES}, k_{NES} are mass, viscous damping and non-linear stiffness coefficients of the NES, respectively; x_1 and x_{NES} are the displacements of the primary structure and the NES, respectively; overdots indicate derivative with respect to time. The assumption of lightweight NES occurs for small values of the mass of the NES (i.e. $\varepsilon = m_{NES}/m_1 << 1$) and it is necessary not only to trigger the passive TET but also for practical issues related to the costs and realisation of the system.

Now consider a MDOF linear system connected to s-NESs through pure cubic stiffness and linear viscous dampers. In this case, the governing equations of motion of the system in its uncontrolled configuration (i.e. with no NESs attached) are:

$$\mathbf{M}\ddot{\mathbf{U}}(t) + \mathbf{C}\dot{\mathbf{U}}(t) + \mathbf{K}\mathbf{U}(t) = \mathbf{f}(t) \tag{2}$$

where $\mathbf{U}(t)$, $\dot{\mathbf{U}}(t)$, $\ddot{\mathbf{U}}(t)$ are the r-dimensional generalised displacement vector and its derivatives, respectively; $\mathbf{M}$, $\mathbf{C}$ and $\mathbf{K}$ are the mass, damping and linear stiffness matrices of the primary system, respectively; $\mathbf{f}(t)$ is the vector of input forces.

When the MDOF structure is equipped with s-NESs, for each of them an additional degree of freedom is added to the controlled system and the equations of motion become:

$$\hat{\mathbf{M}}\ddot{\mathbf{X}}(t) + \hat{\mathbf{C}}\dot{\mathbf{X}}(t) + \hat{\mathbf{K}}\mathbf{X}(t) + \mathbf{F}_{NES}(t) = \hat{\mathbf{f}}(t) \tag{3}$$

in which:

$$\mathbf{X} = \begin{bmatrix} \mathbf{U} \\ \mathbf{X}_{NES} \end{bmatrix} \tag{4}$$

is the n-dimensional generalised displacement vector, being $n = r + s$ the degrees of freedom of the combined system and $\mathbf{X}_{NES}$ the s-dimensional NESs displacement vector. $\hat{\mathbf{M}}$, $\hat{\mathbf{C}}$ and $\hat{\mathbf{K}}$ are the mass, damping and linear stiffness matrices of the controlled system, respectively, and are given as:

$$\hat{\mathbf{M}} = \begin{bmatrix} \mathbf{M} & \mathbf{0} \\ \mathbf{0} & \mathbf{m}_{NES} \end{bmatrix} \quad \hat{\mathbf{C}} = \begin{bmatrix} \mathbf{C} & \mathbf{0} \\ \mathbf{0} & \mathbf{0} \end{bmatrix} + \mathbf{R}\mathbf{c}_{NES}\mathbf{R}^{\mathrm{T}} \quad \hat{\mathbf{K}} = \begin{bmatrix} \mathbf{K} & \mathbf{0} \\ \mathbf{0} & \mathbf{0} \end{bmatrix} \tag{5}$$

where $\mathbf{m}_{NES}$ and $\mathbf{c}_{NES}$ are $(s \times s)$ diagonal matrices containing the individual masses and damping of the NESs devices, respectively. In Equation (5), the matrix $\mathbf{R}$ is the $(n \times s)$ linear transformation matrix returning the s-ranked vector of relative displacements $\mathbf{Y}(t)$ between the mass of each NES and the degree of freedom of the system to which each device is connected:

$$\mathbf{Y}(t) = \mathbf{R}\mathbf{X}(t) \tag{6}$$

Finally, $\mathbf{F}_{NES}$ is the vector collecting all the non-linear forces, that can be expressed, in general, as:

$$\mathbf{F}_{NES}(t) = \mathbf{R}^{\mathrm{T}}\mathbf{f}_{NES}(\mathbf{Y}(t)) \tag{7}$$

where the i-th term of the s-dimensional vector $\mathbf{f}_{NES}(\mathbf{Y}(t))$ is defined as:

$$f_{NES,i}(Y_i(t)) = \hat{k}_{NES,i} Y_i(t)^3 \tag{8}$$

with $\hat{k}_{NES,i}$ the non-linear cubic stiffness of the i-th NES.

2.2 Stochastic linearisation

Among other approximated methods for analysing non-linear random-vibrations problems (e.g. perturbation approaches), the Stochastic Linearisation (SL) is relatively easy to implement, computationally efficient and it has a large range of applicability. This technique has become popular to analyse the performance of non-linear passive control systems to reduce the structural response under random loads, such as Tuned Liquid Column Dampers (Socha 2005, Di Matteo *et al.* 2014) and Fluid Viscous Damper (Guo *et al.* 2002, Di Paola and Navarra 2009). In Oliva *et al.* (2017), an approximate design approach based on the use of the SL technique is proposed for the case of SDOF structures controlled by single NESs and subjected to white noise excitations.

Basically, the SL consists in replacing the non-linear system considered with an equivalent linear one, where the coefficients of the latter system are calibrated by minimising the difference between the two systems in statistical sense (Atalik and Utku 1976). Applying the method to the case at hands, the initial non-linear system in Equation (3) can be replaced with the following:

$$\hat{\mathbf{M}}^{(e)}\ddot{\mathbf{X}}(t) + \hat{\mathbf{C}}^{(e)}\dot{\mathbf{X}}(t) + \hat{\mathbf{K}}^{(e)}\mathbf{X}(t) = \hat{\mathbf{f}}(t) \tag{9}$$

When the primary system is controlled by single or multiple NESs, the equivalent linear mass and damping matrices coincide with those of the nonlinear system , i.e. $\hat{\mathbf{M}}^{(e)} = \hat{\mathbf{M}}$ and $\hat{\mathbf{C}}^{(e)} = \hat{\mathbf{C}}$, thus Equation (9) can be rewritten as:

$$\hat{\mathbf{M}}\ddot{\mathbf{X}}(t) + \hat{\mathbf{C}}\dot{\mathbf{X}}(t) + \hat{\mathbf{K}}^{(e)}\mathbf{X}(t) = \hat{\mathbf{f}}(t) \tag{10}$$

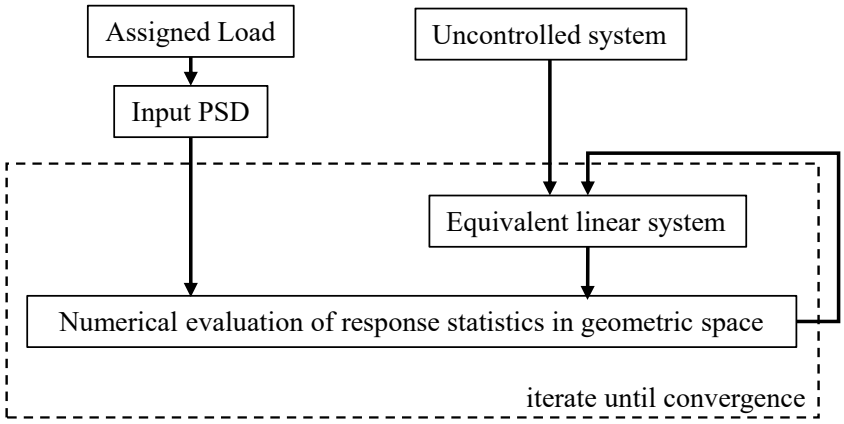

Fig. 2 Flowchart for Statistical Linearisation technique by using the numerical approach.

in which the stiffness matrix $\mathbf{K}^{(e)}$ is defined as:

$$\hat{\mathbf{K}}^{(e)} = \hat{\mathbf{K}} + \mathbf{R}^{\mathrm{T}}\mathbf{D}_{NES}\mathbf{R} \tag{11}$$

In Equation (11), $\mathbf{D}_{NES}$ is the $(s \times s)$ diagonal matrix, whose elements are defined as (Oliva *et al.* 2017):

$$D_{NES,ij} = \mathrm{E}\left[\frac{\partial f_{N,i}}{\partial Y_j}\right] = 3\hat{k}_{NES,i}\sigma^2_{Y_j}\delta_{ij}, \qquad (i,j = 1,2,\ldots,s) \tag{12}$$

where $\sigma^2_{Y_j}$ is the variance of the j-th relative displacement between the i-th NES and the structural node to which it is attached, δ_{ij} is the Kronecker delta and $\mathrm{E}[\cdot]$ stands for ensemble average.

Since the relative displacement Y_j is still unknown, an iterative procedure is required to achieve the solution, as shown in the flowchart reported in Figure 2. In particular, it can be assumed that $\mathbf{D}_{NES}(t)$ is equal to zero at the first iteration of the SL, whereas, at successive iterations, the estimates of equivalent linear matrices $\hat{\mathbf{K}}^{(e)}$ evaluated at the previous iteration are considered. The iterative procedure ends when the differences in estimating $\hat{\mathbf{K}}^{(e)}$ between two subsequent iterations are smaller than a prescribed tolerance.

At each iteration, the variances of relative displacements $\sigma^2_{Y_i}$ or, equivalently, the zero-order spectral moments of the response processes $Y_i(t)$ have to be calculated. Normally, this is done by performing several numerical integrations in the geometric space. 1The m-th order spectral moment matrix can be written as:

$$\lambda_{m,\mathbf{Y}} = \mathbf{R}\left(\int_0^\infty \omega^m \mathbf{G}_{\mathbf{XX}}(\omega)\, d\omega\right)\mathbf{R}^{\mathrm{T}} \tag{13}$$

in which $\mathbf{G}_{\mathbf{XX}}(\omega)$ is the one-sided PSD matrix of the response, i.e.:

$$\mathbf{G}_{\mathbf{XX}}(\omega) = \mathbf{H}^*(\omega)\,\mathbf{G}_{\mathbf{ff}}(\omega)\,\mathbf{H}^{\mathrm{T}}(\omega) \tag{14}$$

In Equation (14), $\mathbf{G_{ff}}(\omega)$ is the input PSD matrix, whereas $\mathbf{H}(\omega)$ is the transfer functions matrix, defined for the case of the equivalent linear system as:

$$\mathbf{H}(\omega) = \left[-\omega^2\hat{\mathbf{M}} + i\omega\hat{\mathbf{C}} + \hat{\mathbf{K}}^{(e)}\right]^{-1} \tag{15}$$

Numerical integration of Equation (13) needs large computational efforts and may lead to inaccurate estimations of spectral moments in the case of low damping values, since very sharp functions are involved. Therefore, depending on the problem under consideration, this approach could be time consuming due to the many numerical integrations to perform, even if it is drastically reduced with reference to Monte Carlo simulations.

3. Efficient stochastic linearisation

In this section, a more efficient procedure to evaluate the spectral moments of the response of classically as well as non-classically damped systems is proposed. This approach allows to avoid most of the burdensome numerical integrations, thus reducing the calculation time.

As well known, the spectral moments are directly related to statistics of stochastic processes, e.g. $\lambda_{0,X}$ and $\lambda_{2,X}$ are respectively the variances of the response process $X(t)$ and of its time derivative. Other quantities, such as central frequency, bandwidth parameter or approximate solutions for the first-passage problem, can be evaluated in terms of the first few spectral moments (Vanmarcke 1972, 1975, Der Kiureghian 1980, Di Paola and Muscolino 1986).

The proposed approach, as shown in Figure 3, consists of the following main steps: a) execution of the generalised modal analysis; b) analytic evaluation of the first direct spectral moments of modal oscillators, once the Power Spectral Density (PSD) functions of the input are known; c) computation of the cross spectral moments in modal decoupled space; d) evaluation in the geometric space of spectral moments of a set of response quantities of interest, obtained as linear combinations of the selected degrees-of-freedom.

In general, the presence of passive control devices makes the equivalent linear system non-classically damped and a generalised modal analysis is required. As customary, the equations of motion of the equivalent system (Eq. (10)) can be reformulated into a set of $2n$ first-order differential equations:

$$\dot{\mathbf{Z}}(t) = \mathbf{D}^{(e)}\mathbf{Z}(t) + \mathbf{V}(t) \tag{16}$$

where the state-variables vector $\mathbf{Z}(t)$, the system matrix $\mathbf{D}^{(e)}$ and the load vector $\mathbf{V}(t)$ are respectively defined as:

$$\mathbf{Z}(t) = \begin{bmatrix} \mathbf{X} \\ \dot{\mathbf{X}} \end{bmatrix}; \quad \mathbf{D}^{(e)} = \begin{bmatrix} \mathbf{0} & \mathbf{I}_n \\ -\hat{\mathbf{M}}^{-1}\hat{\mathbf{K}}^{(e)} & -\hat{\mathbf{M}}^{-1}\hat{\mathbf{C}} \end{bmatrix}; \quad \mathbf{V}(t) = \begin{bmatrix} \mathbf{0} \\ \mathbf{f}(t) \end{bmatrix} \tag{17}$$

being $\mathbf{I}_n$ the $(n \times n)$ identity matrix. The eigenvalues γ_i and the eigenvectors $\boldsymbol{\psi}_i$ of $\mathbf{D}^{(e)}$ occur in conjugate pairs and they are collected to have $\gamma_i = \gamma_{i+n}^*$ and $\boldsymbol{\psi}_i = \boldsymbol{\psi}_{i+n}^*$, denoting

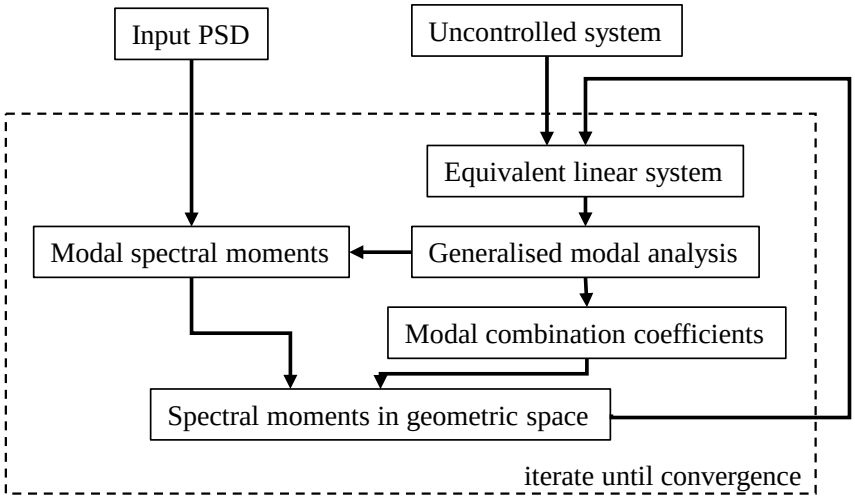

Fig. 3 Flowchart for Statistical Linearisation technique by using the proposed procedure.

with the asterisk the complex conjugate. Due to the structure of the state-variables vector, the i-th eigenvector and the modal matrix are given as:

$$\boldsymbol{\psi_i} = \begin{bmatrix} \boldsymbol{\phi}_i \\ \gamma_i \boldsymbol{\phi}_i \end{bmatrix}, \quad \boldsymbol{\Psi} = \begin{bmatrix} \boldsymbol{\psi}_1 & \boldsymbol{\psi}_2 & \cdots & \boldsymbol{\psi}_{2r} \end{bmatrix} = \begin{bmatrix} \boldsymbol{\Phi} & \boldsymbol{\Phi}^* \\ \boldsymbol{\Gamma}\boldsymbol{\Phi} & \boldsymbol{\Gamma}^*\boldsymbol{\Phi}^* \end{bmatrix} \tag{18}$$

in which $\boldsymbol{\Gamma} = diag\{ \gamma_1, \ \gamma_2, \ \cdots, \ \gamma_n\}$ is the diagonal matrix of the first n eigenvalues and $\boldsymbol{\Phi} = \begin{bmatrix} \boldsymbol{\phi}_1, & \boldsymbol{\phi}_2, & \cdots, & \boldsymbol{\phi}_n \end{bmatrix}$ is the reduced modal matrix in terms of only displacements. The projections of load vector into the modal space are given by $\mathbf{p}(t) = \boldsymbol{\Psi}^{-1}\mathbf{V}(t)$.

Moreover, the i-th eigenvalue can be written with the following notation:

$$\gamma_i = -\zeta_i \, \omega_{0i} \pm i \, \omega_{Di} \tag{19}$$

in which:

$$\omega_{0i} = |\gamma_i|, \quad \zeta_i = -\frac{\mathrm{Re}\,[\gamma_i]}{|\gamma_i|}, \quad \omega_{Di} = \omega_i \sqrt{1 - \zeta_i^2} \tag{20}$$

have the meaning of natural frequency, modal damping and damped frequency of the i-th modal oscillators, respectively.

There is a class of input PSD functions for which it is possible to obtain closed-form evaluations of direct spectral moments in the modal space, without resorting to numerical integrations (Artale *et al.* 2017). For instance, assuming that the input excitation can be approximated by a mono-correlated random process $\mathbf{f}(t) = \boldsymbol{\tau} W(t)$, being $\boldsymbol{\tau}$ the location vector and $W(t)$ a Gaussian and stationary white noise random process having strength G_0, the first direct modal spectral moments of the i-th modal oscillator Q_i can be easily

evaluated by means of the well-known expressions:

$$\begin{aligned}
\lambda_{m,Q_i} &= \frac{\pi G_0}{4\,\zeta_i \omega_{0i}^{3-m}}; && m = 0, 2 \\
\lambda_{1,Q_i} &= \frac{\pi G_0}{4\zeta_i \omega_{0i}^2} \frac{2}{\pi \beta_i} \tan^{-1} \frac{\beta_i}{\zeta_i}; && m = 1 \\
\lambda_{3,Q_i} &= \frac{\pi G_0}{4\zeta_i} \frac{2\left(1 - 2\zeta_i^2\right)}{\pi \beta_i} \tan^{-1} \frac{\beta_i}{\zeta_i}; && m = 3
\end{aligned} \tag{21}$$

where $\beta_i = \sqrt{1 - \zeta_i^2}$.

Di Paola and Muscolino (1988) have demonstrated that the cross-spectral moments of any order λ_{m,Q_j,Q_k}, if they exist for a given input PSD, can be obtained recursively as linear combinations of only the first four order (from 0 to 3) direct spectral moments. In particular, real and imaginary parts of even-order cross-spectral moments can be determined as:

$$\begin{aligned}
\mathrm{Re}\left[\lambda_{m,Q_j,Q_k}\right] &= \frac{(-1)^{m/2}}{2}\left(\lambda_{0,Q_j}\gamma_{m,k,j}\omega_{0j}^2 + \lambda_{2,Qj}\delta_{m,k,j} + \lambda_{0,Q_k}\gamma_{m,j,k}\omega_{0k}^2 + \lambda_{2,Q_k}\delta_{m,j,k}\right) \\
\mathrm{Im}\left[\lambda_{m,Q_j,Q_k}\right] &= \frac{(-1)^{m/2}}{2}\left(\lambda_{1,Q_j}\varepsilon_{m,k,j} - \lambda_{1,Q_k}\varepsilon_{m,j,k} + \lambda_{3,Q_j}\alpha_{m,j,k} - \lambda_{3,Q_k}\alpha_{m,k,j}\right)
\end{aligned} \tag{22}$$

whereas for the odd-order cross-spectral moments:

$$\begin{aligned}
\mathrm{Re}\left[\lambda_{m,Q_j,Q_k}\right] &= \frac{(-1)^{(m+1)/2}}{2}\left(\lambda_{1,Q_j}\varepsilon_{m,k,j} + \lambda_{1,Q_k}\varepsilon_{m,j,k} + \lambda_{3,Q_j}\alpha_{m,k,j} + \lambda_{3,Q_k}\alpha_{m,j,k}\right) \\
\mathrm{Im}\left[\lambda_{m,Q_j,Q_k}\right] &= \frac{(-1)^{(m-1)/2}}{2}\left(\lambda_{0,Q_j}\gamma_{m,k,j}\omega_{0j}^2 + \lambda_{2,Q_j}\delta_{m,k,j} - \lambda_{0,Q_k}\gamma_{m,j,k}\omega_{0k}^2 - \lambda_{2,Q_k}\delta_{m,j,k}\right)
\end{aligned} \tag{23}$$

In Equations (22) and (23), the following positions have been made:

$$\begin{aligned}
\alpha_{m,j,k} &= \alpha_{m-1,j,k} + \omega_{Dk}\beta_{m-1,j,k}; \\
\beta_{m,j,k} &= -\zeta_k\,\omega_{0k}\,\beta_{m-1,j,k} - \omega_{Dk}\alpha_{m-1,j,k}; \\
\gamma_{m,j,k} &= \zeta_k\omega_{0k}\alpha_{m,j,k} + \omega_{Dk}\beta_{m,j,k}; \\
\delta_{m,j,k} &= \zeta_k\omega_{0k}\alpha_{m,j,k} - \omega_{Dk}\beta_{m,j,k}; \\
\varepsilon_{m,j,k} &= 2\zeta_k\omega_k\omega_{Dk}\beta_{m,j,k} + \alpha_{m,j,k}\left(\omega_{0k}^2 - 2\omega_{Dk}^2\right);
\end{aligned} \tag{24}$$

being:

$$\begin{aligned}
\alpha_{0,j,k} &= 4\left(\zeta_j\omega_j + \zeta_k\omega_k\right)/K_{jk} \\
\beta_{0,j,k} &= 2\left(\omega_{0j}^2 - \omega_{0k}^2 + 2\zeta_j\zeta_k\omega_{0j}\omega_{0k} + 2\zeta_k^2\omega_{0k}^2\right)/\left(\omega_{Dk}K_{jk}\right) \\
K_{jk} &= \left(\omega_{0j}^2 - \omega_{0k}^2\right)^2 + 4\zeta_j\zeta_k\left(\omega_{0j}^2 + \omega_{0k}^2\right)\omega_{0j}\omega_{0k} + 4\left(\zeta_j^2 + \zeta_k^2\right)\omega_{0j}^2\omega_{0k}^2
\end{aligned} \tag{25}$$

Once the cross-spectral moments of the modal oscillators are determined, the spectral moments of the r-th element of the set of quantities of interest in the geometric space defined by the vector $\mathbf{Y}$ can be computed as (Igusa *et al.* 1984):

$$\lambda_{m,Y_r} = \sum_{j=1}^{\hat{n}} \sum_{k=1}^{\hat{n}} \left(C_{r,jk} \mathrm{Re}\left[\lambda_{m,Q_j,Q_k}\right] - D_{r,jk} \mathrm{Im}\left[\lambda_{m+1,Q_j,Q_k}\right] + E_{r,jk} \mathrm{Re}\left[\lambda_{m+2,Q_j,Q_k}\right] \right) \quad (26)$$

where the modal combination coefficients $C_{r,jk}$, $D_{r,jk}$ and $E_{r,jk}$ can be obtained as:

$$C_{r,jk} = a_{rj} a_{rk}; \quad D_{r,jk} = a_{rj} c_{rk} - a_{rk} c_{rj}; \quad E_{r,jk} = c_{rj} c_{rk} \quad (27)$$

being a_{rj} and c_{rj} the entries of the following matrices:

$$\mathbf{a} = -2\mathrm{Re}\left[\mathbf{b}\boldsymbol{\Gamma}^*\right]; \quad \mathbf{c} = -2\mathrm{Re}\left[\mathbf{b}\right]; \quad \mathbf{b} = \mathbf{R}\boldsymbol{\Phi}\mathbf{P}_{\hat{n}} \quad (28)$$

with $\mathbf{P}_{\hat{n}} = diag\{ \ P_1, \ \ P_2, \ \ \cdots, \ \ P_{\hat{n}}\}$.

The proposed method is easy to implement in actual computing programs and allows to speed up procedures that make intense use of the stochastic analyses, such as SL approaches and optimisation problems. In order to show its benefits, numerical applications are reported in the following section.

4. Numerical application

Although there are several studies focused on the NES, the design of the latter is still challenging because of its complex dynamic behaviour and its sensitivity to loading perturbations. Closed-form solutions to determine the optimal nonlinear stiffness of the NES have been derived mainly for deterministic loads (Starosvetsky and Gendelman 2008, Nguyen and Pernot 2012). Conversely, in presence of random excitations the design of the NES has been carried out by means of burdensome Monte carlo simulations (Oliva *et al.* 2017). Herein, the proposed efficient linearisation technique is applied as alternative method for evaluating the NES parameters (i.e. nonlinear stiffness and linear damping) and its ability to mitigate the structural response of a flexible wing, allowing for a significant reduction of the computation time.

A case study provided by Hubbard *et al.* (2010) has been selected as numerical application. It consists of a uniform-thickness, 6061-T6 aluminium alloy model wing with attached a NES located in the mid-chord of the wingtip. The dimensions of the wing, the clumped boundary conditions and the NES locations are reported in Figure 4-a.

The equations of motion of the wing in its uncontrolled (i.e. without NES) and controlled (i.e. with NES) configurations are given respectively by Equations (2) and (3), in which stiffness and mass matrices of the wing, $\mathbf{M}$ and $\mathbf{K}$, have been obtained by means of the FE method. In particular, the wing has been discretized by using 4-nodes linear shell elements with a 8×32 mesh and a total of 297 nodes and 891 degrees of freedom. Figure 4-b depicts a representation of the FE model. The load is modelled as a transversal mono-correlated white noise equally acting on all the model nodes having a PSD amplitude equal to $G_0 = 2 \cdot 10^{-6}$ N^{2}s/rad, which corresponds to a total transversal force whose peak value is about 7 kN.

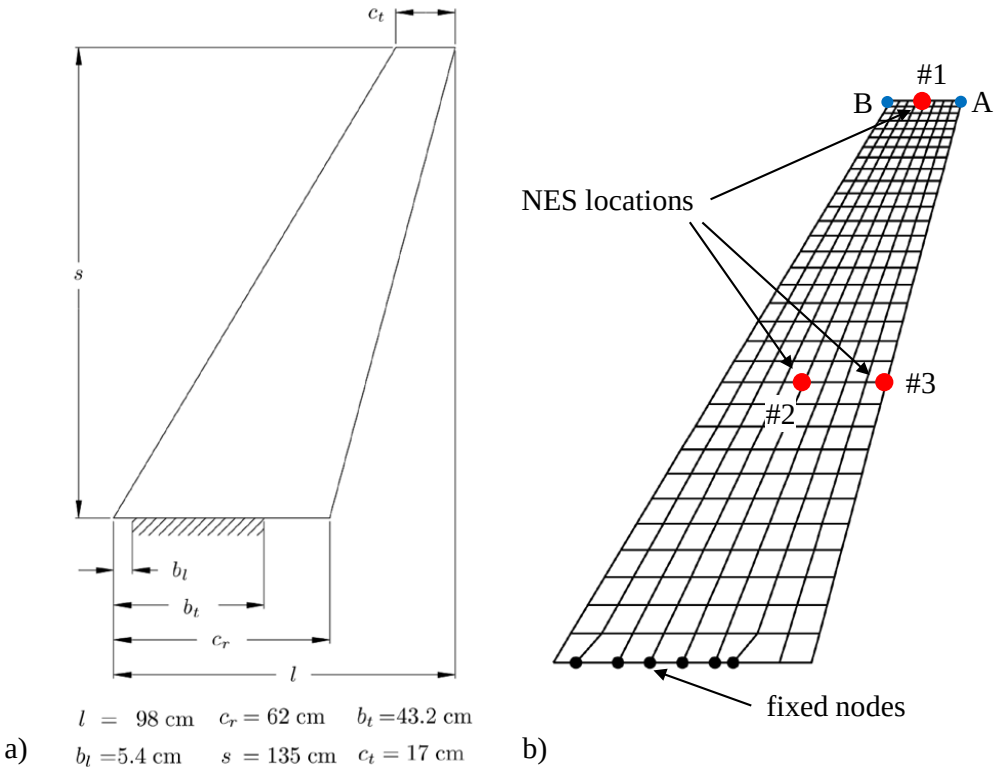

Fig. 4 Wing model from Hubbard *et al.* (2010); a) dimensions, boundary conditions and NES location (red dot); b) mesh used in FE model, fixed nodes (black dots) and NES location (red dot).

4.1 Validation in terms of accuracy and computational time

Since the proposed procedure differs from classical SL mainly in the way the response statistics are computed, it is worth to emphasize the differences between the two methods in terms of both accuracy and computational time. In the present case, the input load is modelled as a Gaussian white noise with assigned PSD amplitude, and the response statistics of each modal oscillator are known in closed exact form (Equation (21)). Consequently, the proposed procedure leads to exact values of the system response statistics. On the other hand, the numerical integration of Equation (13) is needed in classical SL procedures. In this case, the evaluation of response statistics will depend on the frequency discretization interval and when it is too large, it leads to inaccurate estimations of the spectral moments specially in the case of low damped systems whose elements of the transfer functions matrix $\mathbf{H}(\omega)$ are very sharp.

Table 1 reports the response statistics in terms of variance of the rightmost point of the wingtip (point A in Figure 4), with reference to the wing model in its uncontrolled state, for the proposed method and for the classic numeric stochastic analysis. Analyses have been carried out for three different frequency ranges, namely $[0 \div 2500]$ rad/s, $[0 \div 1250]$ rad/s

Table 1 Computational times and relative errors for application of numerical and analytical procedures.

$\Delta\omega$	Computational time [s]			$\sigma^2_{A,U}$	relative error
	$[0 \div 2500]$ rad/s	$[0 \div 1250]$ rad/s	$[0 \div 500]$ rad/s	[cm^2]	[%]
2.000	11.088	5.688	2.186	0.3410	-38.18
1.250	17.843	9.050	3.563	0.6926	25.55
1.000	21.590	11.679	4.463	0.5720	3.69
0.800	27.802	13.650	5.504	0.5136	-6.90
0.625	34.823	17.493	7.229	0.5652	2.46
0.500	43.597	21.707	8.834	0.5474	-0.77
0.400	55.302	27.346	11.071	0.5531	0.26
0.3125	69.891	34.843	14.118	0.5518	0.02
0.250	87.521	44.087	17.480	0.5517	0.00
Analytical		0.556		0.5516	

and $[0 \div 500]$ rad/s and for several frequency discretization steps. These frequency ranges have been selected in order to include the contributions of the first 18, 11 and 5 modes, respectively, established that the cumulative modal mass participating ratios are 90.2%, 88.2% and 83.8%, respectively.

It resulted that, in the present case, the accuracy mainly depends on the discretization step and very close results have been obtained by varying the frequency range.

Moreover, it is worth to stress that in order to achieve a good approximation (with negligible errors) of the response statistics for the case under examination, it is necessary to choose a discretization of frequency $\Delta\omega = 0.25$ rad/s or lower, thus resulting in increased computational efforts.

The performance of the proposed procedure in terms of computational time has been also investigated. All numerical procedure have been implemented in MATLAB environment and executed on a personal computer with Intel i7-6700HQ quad core processor @2.60GHz and 16 GB DDR-4 RAM. In Table 1, the computational times are reported for each analysis and it is worth to note that, by using the proposed analytical procedure, the computational time can be tremendously reduced with respect to the classical numerical procedures.

Moreover, when the input is not a white Gaussian process and the response statistics of the modal oscillators are not known in closed form, the proposed procedure allows a drastic reduction of the computational time. In fact, assuming that a modal truncation is applied and the first $\hat{n} < n$ modal contributions are retained, only $4\hat{n}$ numerical integrations in the modal space are needed with respect to $n \times n$ numerical integrations in the geometric space.

Obviously, when performing a complete SL, both proposed method and classic numeric stochastic analysis need the same number of iterations to converge (Navarra *et al.* 2020b, a) and the overall computational time will increase proportionally. Furthermore, when dealing with optimal design procedures, both computational time and memory demand can become a serious issue that, in the case of the classical SL procedures, could compromise the success

of the analysis.

4.2 Optimal design of a NES device

In order to design a NES able to suppress wing vibrations and evaluate its performance, the non-linear system in Equation (3) has been replaced with the equivalent linear equation (10) and the proposed method has been used at each iteration of the optimisation procedure.

In this regard, the NES location #1 in Figure 4 has been selected and two performance indices have been defined as the percentage ratio of standard deviations of the controlled and uncontrolled systems. In particular, the index η_1 is related to the transversal displacements at the rightmost point of the wingtip (point A in Figure 4-b) and takes into account of the flexural behaviour of the wing model, whereas the index η_2 considers the torsional rotation measured from the differential transversal displacements of the points A and B in Figure 4-b. The analytic expressions of the performance indices are:

$$\eta_1 = 100 \cdot \frac{\sigma_{A,C}}{\sigma_{A,U}}; \quad \eta_2 = 100 \cdot \frac{\sigma_{\varphi,C}}{\sigma_{\varphi,U}} \tag{29}$$

in which the subscripts C and U stand for controlled and uncontrolled configurations, respectively, and:

$$\varphi_S = \frac{w_{A,S} - w_{B,S}}{c_t} \quad (S = C, U) \tag{30}$$

is the tosional rotation, being w the transversal displacements and c_t the wingtip chord length (Figure 4-a).

The minimisation procedure has been carried out by using the routine *fminsearch* in MATLAB environment that uses the simplex search method developed by Lagarias *et al.* (1998). This is a direct search method that does not use numerical or analytic gradients.

Figure 5 shows a contour plot of the index η_1 against the design parameters of the NES, $\hat{k}_{NES}$ and c_{NES}, for a given input strength $G_0 = 2 \cdot 10^{-6}$ N^{2}s/rad and by assuming a NES mass ratio $\varepsilon = 0.02$. This figure reports also the optimal search path and the numerical values of the optimal NES parameters. Since the performance factor η_1 is defined so that the lower its value the higher the effectiveness of the NES, it is possible to affirm that the NES designed by using the proposed method allows for a considerable reduction of the standard deviation of the displacements of the wingtip, which stands of about 60%.

Figure 5 shows also that the use of the NESs as vibration absorbers leads to a robust control. In fact, for a given input strength, the performance index function presents a very large flat zone in the neighbourhood of the optimal point, thus meaning that the control is assured even if large deviations from the NES device optimal parameters occur.

Unlike linear vibration absorbers, the efficiency of the NES is strongly dependent on the intensity of the load to which the structure is subject. Hence, a sensitivity analysis has been performed, in which the optimal non-linear stiffness $\hat{k}_{NES,opt}$ has been recalculated for any change of the white noise PSD amplitude G_0, ranging from $5 \cdot 10^{-7}$ to 10^{-4} N^{2}s/rad.

Figure 6 reports the effects of the variation of the amplitude of the white noise load on the optimal cubic stiffness $\hat{k}_{NES,opt}$ for different values of the mass ratio ε of the NES device. Values of ε less than 10% have been considered in order to respect the assumption of

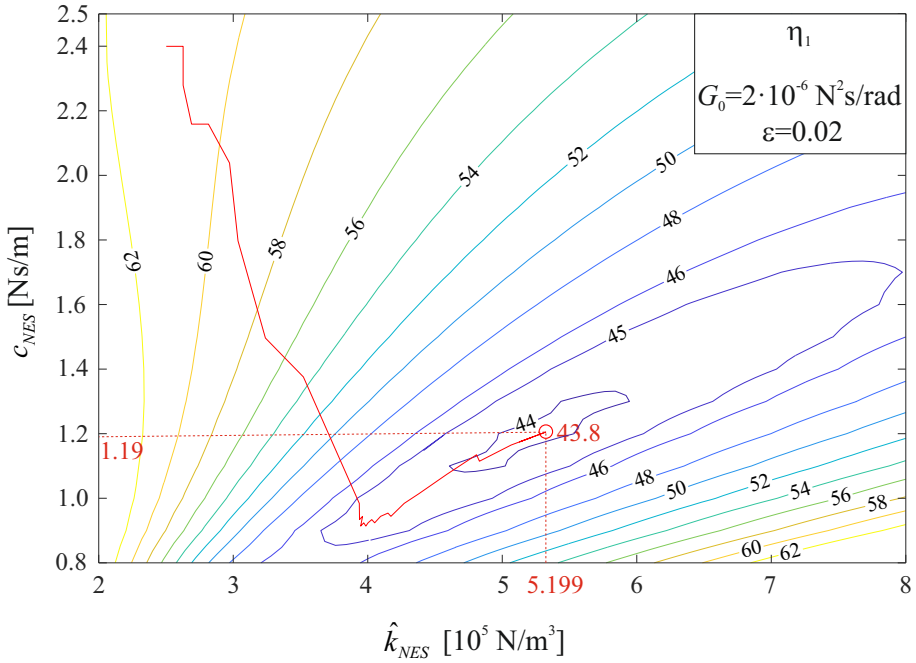

Fig. 5 Performance index η_1 against NES design parameters for $G_0 = 2 \cdot 10^{-6}$ $\mathrm{N^2\,s/rad}$ and $\varepsilon = 0.02$. Optimal search path (red line) and optimal parameters $\hat{k}_{NES} = 5.199 \cdot 10^5\,\mathrm{N/m^3}$ and $c_{NES} = 1.19\,\mathrm{N\,s/m}$.

lightweight NES. The results of the several numerical optimisations show that the optimal non-linear stiffness increases increasing the mass ratio, whereas it decreases increasing the amplitude of G_0. Conversely, the optimal values of NES damping and the corresponding performance index, as reported in Table 2, depend only on the mass ratio. This seems to confirm what has been already demonstrated by Oliva *et al.* (2017). In their work, that is related to the response of civil structures equipped with NESs to base loadings, it has been proven that the optimal non-linear stiffness is inversely proportional to the amplitude of the PSD function of the white noise both using an approach based on the SL technique as well as an approach based on the numerical results of a MCSs campaign.

The last numerical application is devoted to compute the performance of the NES when

Table 2 Optimal damping and performance index for varying NES mass ratio.

ε	$c_{NES,opt}$ [Ns/m]	η_{opt}
1%	0.447	50.69%
2%	1.192	43.82%
5%	4.005	35.56%
10%	9.096	30.02%

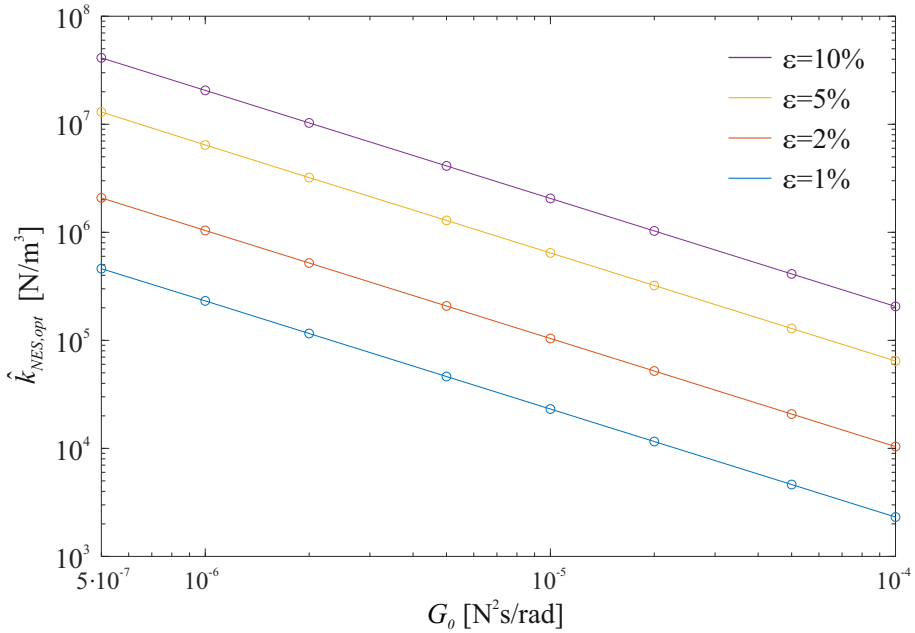

Fig. 6 Optimal cubic stiffness against input strength G_0 for different values of NES mass ratio.

its location is varied and its optimal design is carried out by minimising the two performance indices η_1 and η_2. In particular, the three NES locations reported in Figure 4-b have been investigated for two different values of mass ratio $\varepsilon = 0.01$ and $\varepsilon = 0.02$ and the results are collected in Table 3.

Since the dynamic behaviour of the wing model is dominated by the first mode, the best control performance is achieved when NES is the location #1 and no significant differences are noticed when using the two performance indices. Theses result also confirm that the larger the value of the mass ratio, the greater the reduction in the controlled response.

5. Conclusions

Given the strong dependence of the cubic stiffness of NES on loading conditions and its complex non-linear behaviour, its design is complicated and often requires the use of very time-consuming techniques (e.g. Monte Carlo simulations). In this paper, an easy-to-implement and efficient method for the optimal design of the non-linear passive control device NES has been proposed into a probabilistic framework.

Firstly, a general Stochastic Linearisation approach for MDOF structural systems controlled by multi NES devices has been introduced. It consists in replacing the non-linear governing equations of the combined system with an equivalent linear one. However, depending on the problem under consideration, the SL could be time consuming due to the many numerical integrations required to obtain the solution, even if the computational effort is drastically reduced with reference to Monte Carlo simulations.

Table 3 Comparison among optimal design of NES in different locations and for different performance indices.

		$\varepsilon = 0.01$			$\varepsilon = 0.02$		
		$\hat{k}_{NES,opt}$	$c_{NES,opt}$	η_{opt}	$\hat{k}_{NES,opt}$	$c_{NES,opt}$	η_{opt}
NES location #1	η_1	115687	0.447	50.69%	519926	1.190	43.82%
	η_2	114194	0.452	51.79%	508481	1.186	44.86%
NES location #2	η_1	571557	0.704	85.13%	1070393	1.108	73.49%
	η_2	621164	0.721	85.79%	1066587	1.104	73.72%
NES location #3	η_1	400869	0.649	80.26%	765511	0.992	67.17%
	η_2	444751	0.694	81.69%	779294	0.960	68.38%

The proposed methodology, instead, leads to the following advantages:

- At each iteration step of the SL, the first spectral moments of the response in the geometric space can be quickly evaluated without resorting or, in general, strongly reducing the use of numerical integrations;
- it applies for both classically and not-classically damped systems and can be easily implemented into a standard stochastic analysis program routine;
- it leads to drastic reduction of the computational burden with respect to the classic stochastic analysis. If used inside a SL algorithm, the reduction in computational time is proportional to the number of required iterations.

The applicability of the proposed approach has been shown through numerical applications on the design of a NES able to mitigate the vibrations of a flexible wing, modelled as mono-correlated white noise processes. The following conclusions can be drawn:

- NESs can be used as passive control devices since they allow for a large reduction of wing vibrations. Moreover, a robust control is assured even if large deviations from the NES device optimal parameters occur;
- by means of a numerical optimization procedure the optimal NES parameters have been obtained for three assumed NES locations and for two different objective functions, related to flexural and torsional behaviour of the wing. It has been confirmed that the NES located at the wingtip is the most effective in reducing the out-of-plane vibrations.
- A parametric analysis have been performed by varying the input strength and the NES mass ratio. The results confirmed that optimal values of the non-linear stiffness increase when the device mass increases and decrease when the input strength increases, whereas the optimal NES damping depends only on the device mass.

References

Artale, V., Navarra, G., Ricciardello, A. and Barone, G. (2017), "Exact closed-form fractional spectral moments for linear fractional oscillators excited by a white noise", *ASCE-ASME J Risk Uncertainty, Part B*, **3**(3), https://doi.org/10.1115/1.4036700.

Atalik, T.S. and Utku, S. (1976), "Stochastic Linearization of Multi-Degree-of-Freedom Nonlinear System", *Earthq. Eng. Struct. D.*, **4**(March 1975), 411–420, https://doi.org/10.1002/eqe.4290040408.

Barone, G., Lo Iacono, F., Navarra, G. and Palmeri, A. (2019), "Closed-form stochastic response of linear building structures to spectrum-consistent seismic excitations", *Soil Dyn. Earthq. Eng.*, **125**, 105724, https://doi.org/10.1016/j.soildyn.2019.105724.

Bergeot, B., Bellizzi, S. and Cochelin, B. (2016), "Passive suppression of helicopter ground resonance instability by means of a strongly nonlinear absorber", *Adv.Aircraft Spacecraft Sci.*, **3**(3), 271–298, https://doi.org/10.12989/aas.2016.3.3.271.

Der Kiureghian, A. (1980), "Structural response to stationary excitation", *J. Eng. Mech.-ASCE*, **106**(6), 1195–1213.

Di Matteo, A., Lo Iacono, F., Navarra, G. and Pirrotta, A. (2014), "Direct evaluation of the equivalent linear damping for TLCD systems in random vibration for pre-design purposes", *Int. J. Nonlinear Mech.*, **63**, 19–30, https://doi.org/10.1016/j.ijnonlinmec.2014.03.009.

Di Paola, M. and Muscolino, G. (1986), "On the convergent parts of high order structural responses", *J. Sound Vib.*, **110**, 233–245, https://doi.org/10.1016/S0022-460X(86)80207-3.

Di Paola, M. and Muscolino, G. (1988), "Analytic evaluation of spectral moments", *J. Sound Vib.*, **124**(3), 479–488, https://doi.org/10.1016/S0022-460X(88)81389-0.

Di Paola, M. and Navarra, G. (2009), "Stochastic seismic analysis of MDOF structures with nonlinear viscous dampers", *Struct. Control Hlth.*, **16**(3), 303–318, https://doi.org/10.1002/stc.254.

Elishakoff, I. (2000), "Stochastic linearization technique: a new interpretation and a selective review", *Shock Vib.*, **32**, 179–188, https://doi.org/10.1177/058310240003200301.

Gendelman, O. (2001), "Transition of Energy to a Nonlinear Localized Mode in a Highly Asymmetric System of Two Oscillators", *Nonlinear Dynam.*, **25**(1/3), 237–253, https://doi.org/10.1023/A:1012967003477.

Gendelman, O., Manevitch, L., Vakakis, A. and M'Closkey, R. (2001), "Energy Pumping in Nonlinear Mechanical Oscillators: Part I - Dynamics of the Underlying Hamiltonian Systems", *J. Appl. Mech.*, **68**(1), 34, https://doi.org/10.1115/1.1345524.

Gendelman, O.V. (2008), "Targeted energy transfer in systems with non-polynomial nonlinearity", *J. Sound Vib.*, **315**(3), 732–745, https://doi.org/10.1016/j.jsv.2007.12.024.

Gendelman, O.V., Sapsis, T., Vakakis, A.F. and Bergman, L.A. (2011), "Enhanced passive targeted energy transfer in strongly nonlinear mechanical oscillators", *J. Sound Vib.*, **330**(1), 1–8, https://doi.org/10.1016/j.jsv.2010.08.014.

Gendelman, O.V., Sigalov, G., Manevitch, L.I., Mane, M., Vakakis, A.F. and Bergman, L.A. (2012), "Dynamics of an Eccentric Rotational Nonlinear Energy Sink", *J. Appl. Mech.*, **79**(1), 011012, https://doi.org/10.1115/1.4005402.

Gourdon, E., Alexander, N., Taylor, C., Lamarque, C. and Pernot, S. (2007), "Nonlinear energy pumping under transient forcing with strongly nonlinear coupling: Theoretical and experimental results", *J. Sound Vib.*, **300**(3-5), 522–551, https://doi.org/10.1016/j.jsv.2006.06.074.

Guo, A., Xu, X.L. and Wu, B. (2002), "Seismic reliability analysis of hysteretic structure with viscoelastic dampers", *Eng. Struct.*, **24**, 373–383, https://doi.org/10.1016/S0141-0296(01)00103-1.

Hubbard, S.A., McFarland, D.M., Bergman, L.A. and Vakakis, A.F. (2010), "Targeted Energy Transfer Between a Model Flexible Wing and Nonlinear Energy Sink", *J. Aircraft*, **47**(6), 1918–1931, https://doi.org/10.2514/1.C001012.

Igusa, T., Der Kiureghian, A. and Sackman, J.L. (1984), "Modal decomposition method for stationary response of non-classically damped systems", *Earthq. Eng. Struct. D.*, **12**(1), 121–136, https://doi.org/10.1002/eqe.4290120109.

Kerschen, G., Lee, Y., Vakakis, A., McFarland, D. and Bergman, L. (2005), "Irreversible Passive Energy Transfer in Coupled Oscillators with Essential Nonlinearity", *SIAM J. Appl. Math.*, **66**(2), 648–679, https://doi.org/10.1137/040613706.

Kerschen, G., McFarland, D., Kowtko, J., Lee, Y., Bergman, L. and Vakakis, A. (2007), "Experimental demonstration of transient resonance capture in a system of two coupled oscillators with essential stiffness nonlinearity", *J. Sound Vib.*, **299**(4), 822–838, https://doi.org/10.1016/j.jsv.2006.07.029.

Lagarias, J., Reeds, J., Wright, M. and Wright, P. (1998), "Convergence Properties of the Nelder-Mead Simplex Method in Low Dimensions", *SIAM J. Optimiz.*, **9**(1), 112–147, https://doi.org/10.1137/S1052623496303470.

Lee, Y., Kerschen, G., McFarland, D., Hill, W., Nichkawde, C., Strganac, T., Bergman, L. and Vakakis, A. (2007a), "Suppressing Aeroelastic Instability Using Broadband Passive Targeted Energy Transfers, Part 2: Experiments", *AIAA J.*, **45**(10), 2391–2400, https://doi.org/10.2514/1.28300.

Lee, Y., Kerschen, G., Vakakis, A., Panagopoulos, P., Bergman, L. and McFarland, D. (2005), "Complicated dynamics of a linear oscillator with a light, essentially nonlinear attachment", *Physica D*, **204**(1-2), 41–69, https://doi.org/10.1016/j.physd.2005.03.014.

Lee, Y., Vakakis, A., Bergman, L., McFarland, D. and Kerschen, G. (2007b), "Suppression Aeroelastic Instability Using Broadband Passive Targeted Energy Transfers, Part 1: Theory", *AIAA J.*, **45**(3), 693–711, https://doi.org/10.2514/1.24062.

Lee, Y., Vakakis, A., Bergman, L., McFarland, D., Kerschen, G., Nucera, F., Tsakirtzis, S. and Panagopoulos, P. (2008a), "Passive non-linear targeted energy transfer and its applications to vibration absorption: a review", in "Proceedings of the Institution of Mechanical Engineers, Part K: Journal of Multi-body Dynamics", volume 222, pages 77–134, https://doi.org/10.1243/14644193JMBD118.

Lee, Y.S., Vakakis, a.F., Bergman, L.a., McFarland, D.M. and Kerschen, G. (2008b), "Enhancing the Robustness of Aeroelastic Instability Suppression Using Multi-Degree-of-Freedom Nonlinear Energy Sinks", *AIAA J.*, **46**(6), 1371–1394, https://doi.org/10.2514/1.30302.

Lee, Y.S., Vakakis, A.F., Bergman, L.A. and Michael McFarland, D. (2006), "Suppression of limit cycle oscillations in the van der Pol oscillator by means of passive non-linear energy sinks", *Struct. Control Hlth.*, **13**(1), 41–75, https://doi.org/10.1002/stc.143.

McFarland, D., Bergman, L. and Vakakis, A. (2005), "Experimental study of non-linear energy pumping occurring at a single fast frequency", *Int. J. Nonlinear Mech.*, **40**(6), 891–899, https://doi.org/10.1016/j.ijnonlinmec.2004.11.001.

Navarra, G., Lo Iacono, F. and Oliva, M. (2020a), "An Efficient Stochastic Linearisation Procedure for the Seismic Optimal Design of Passive Control Devices", *Front. Built Env.*, **6**, 32, URL https://www.frontiersin.org/article/10.3389/fbuil.2020.00032, https://doi.org/10.3389/fbuil.2020.00032.

Navarra, G., Lo Iacono, F., Oliva, M. and Cascone, D. (2020b), "Speeding up the stochastic linearisation for systems controlled by non-linear passive devices", *Lecture Notes in Mechanical Engineering*, pages 1625–1644, conference of 24th Conference of the Italian Association of Theoretical and Applied Mechanics, AIMETA 2019 ; Conference Date: 15 September 2019 Through 19 September 2019; Conference Code:238859, https://doi.org/10.1007/978-3-030-41057-5_131.

Nguyen, T.A. and Pernot, S. (2012), "Design criteria for optimally tuned nonlinear energy sinkspart

1: transient regime", *Nonlinear D.*, **69**(1-2), 1–19, https://doi.org/10.1007/s11071-011-0242-9.

Nucera, F., Lo Iacono, F., McFarland, D., Bergman, L. and Vakakis, A. (2008), "Application of broadband nonlinear targeted energy transfers for seismic mitigation of a shear frame: Experimental results", *Journal of Sound and Vibration*, **313**(1-2), 57–76, https://doi.org/10.1016/j.jsv.2007.11.018.

Nucera, F., Vakakis, A., McFarland, D., Bergman, L. and Kerschen, G. (2007), "Targeted energy transfers in vibro-impact oscillators for seismic mitigation", *Nonlinear D.*, **50**(3), 651–677, https://doi.org/10.1007/s11071-006-9189-7.

Oliva, M., Barone, G. and Navarra, G. (2017), "Optimal design of Nonlinear Energy Sinks for SDOF structures subjected to white noise base excitations", *Eng. Struct.*, **145**, 135–152, https://doi.org/10.1016/j.engstruct.2017.03.027.

Roberts, J.B. and Spanos, P.D. (2003), *Random vibration and statistical linearization*, Dover, Mineola, NY, USA.

Sapsis, T.P., Dane Quinn, D., Vakakis, A.F. and Bergman, L.a. (2012), "Effective Stiffening and Damping Enhancement of Structures With Strongly Nonlinear Local Attachments", *J. Vib. Acoust.*, **134**(1), 011016, https://doi.org/10.1115/1.4005005.

Sigalov, G., Gendelman, O.V., AL-Shudeifat, M.A., Manevitch, L.I., Vakakis, A.F. and Bergman, L.A. (2012), "Resonance captures and targeted energy transfers in an inertially-coupled rotational nonlinear energy sink", *Nonlinear D.*, **69**(4), 1693–1704, https://doi.org/10.1007/s11071-012-0379-1.

Socha, L. (2005), "Linearization in Analysis of Nonlinear Stochastic Systems: Recent ResultsPart I: Theory", *Appl. Mech. Rev.*, **58**(3), 178, https://doi.org/10.1115/1.1896368.

Starosvetsky, Y. and Gendelman, O. (2008), "Attractors of harmonically forced linear oscillator with attached nonlinear energy sink. II: Optimization of a nonlinear vibration absorber", *Nonlinear D.*, **51**(1-2), 47, https://doi.org/10.1007/s11071-006-9168-z.

Vakakis, A., Gendelman, O., Bergman, L., McFarland, D., Kerschen, G. and Lee, Y. (2009), *Nonlinear Targeted Energy Transfer in Mechanical and Structural Systems*, volume 156 of *Solid Mechanics and Its Applications*, Springer Netherlands, https://doi.org/10.1007/978-1-4020-9130-8.

Vakakis, A.F. (2001), "Inducing Passive Nonlinear Energy Sinks in Vibrating Systems", *J Vib.Acoust.*, **123**(3), 324, https://doi.org/10.1115/1.1368883.

Vanmarcke, E.H. (1972), "Properties of spectral moments with applications to random vibration", *J. Eng. Mech. ASCE*, **98**(2), 425–446.

Vanmarcke, E.H. (1975), "On the Distribution of the First-Passage Time for Normal Stationary Random Processes", *J. Appl. Mech.*, **42**(1), 215, https://doi.org/10.1115/1.3423521.

Wang, J., Wierschem, N., Spencer, B. and Lu, X. (2015a), "Experimental study of track nonlinear energy sinks for dynamic response reduction", *Eng. Struct.*, **94**, 9–15, https://doi.org/10.1016/j.engstruct.2015.03.007.

Wang, J., Wierschem, N., Spencer, B. and Lu, X. (2015b), "Track Nonlinear Energy Sink for Rapid Response Reduction in Building Structures", *J. Eng. Mech. ASCE*, **141**(1), 04014104, https://doi.org/10.1061/(ASCE)EM.1943-7889.0000824.

CC